Watson–Crick base-pairing properties of bicyclo-DNA

Martin Bolli[+], Huldreich U. Trafelet and Christian Leumann*

Department of Chemistry and Biochemistry, University of Bern, Freiestrasse 3, CH-3012 Bern, Switzerland

ABSTRACT

A series of sequences of the DNA analog bicyclo-DNA, 6–12 nucleotides in length and containing all four natural nucleobases, were prepared and their Watson–Crick pairing properties with complementary RNA and DNA, as well as in its own series, were analyzed by UV-melting curves and CD-spectroscopy. The results can be summarized as follows: bicyclo-DNA forms stable Watson–Crick duplexes with complementary RNA and DNA, the duplexes with RNA generally being more stable than those with DNA. Pyrimidine-rich bicyclo-DNA sequences form duplexes of equal or slightly increased stability with DNA or RNA, whereas purine-rich sequences show decreased affinity to complementary DNA and RNA when compared with wild-type (DNA–DNA, DNA–RNA) duplexes. In its own system, bicyclo-DNA prefers antiparallel strand alignment and strongly discriminates for base mismatches. Duplexes are always inferior in stability compared with the natural ones. A detailed analysis of the thermodynamic properties was performed with the sequence 5′-GGATGGGAG-3′·5′-CTCCCATCC-3′ in both backbone systems. Comparison of the pairing enthalpy and entropy terms shows an enthalpic advantage for DNA association ($\Delta\Delta H = -18$ kcal·mol^{-1}) and an entropic advantage for bicyclo-DNA association ($\Delta\Delta S = 49$ cal·K^{-1}·mol^{-1}), leading to a $\Delta\Delta G^{25\,^\circ C}$ of -3.4 kcal·mol^{-1} in favor of the natural duplex. The salt dependence of T_m for this sequence is more pronounced in the case of bicyclo-DNA due to increased counter ion screening from the solvent. Furthermore bicyclo-DNA sequences are more stable towards snake venom phosphodiesterase by a factor of 10–20, and show increased stability in fetal calf serum by a factor of 8 compared with DNA.

INTRODUCTION

Oligonucleotide analogs, displaying strong and sequence specific binding to single-stranded RNA or double-stranded DNA and exhibiting resistance to enzymatic degradation are potential candidates for therapeutic applications as inhibitors of protein expression (1–4). Among the whole family of DNA analogs, those containing defined structural modifications in the sugar–phosphate part gain special interest since the study of their supramolecular interactions can also contribute to the understanding of the structural and energetic factors that define order mode and specificity in DNA association. Within this context we recently introduced the DNA-analog 'bicyclo-DNA' (Fig. 1). This analog was initially designed to stabilize complex formation with complementary natural nucleic acids entropically by exhibiting a higher degree of preorganisation of its single strands for duplex formation due to the conformationally locked sugar structure of the underlying bicyclo-deoxynucleosides (Fig. 1; ref. 5).

We have demonstrated that decamers of bicyclo-deoxyadenosine [bcd(A$_{10}$)] and bicyclothymidine [bcd(T$_{10}$)] bind to their natural RNA and DNA complements as well as with each other, forming double and triple helical structures. Compared with natural DNA, duplex formation is associated with (numerically) reduced pairing enthalpy and entropy terms, having compensatory effects on the free energy of duplex formation (6,7). Complexes of bcd(A$_{10}$) with complementary DNA or RNA are thermodynamically more stable than those of bcd(T$_{10}$).

Structural investigations on the mononucleoside (5) and dinucleotide (8) level by temperature dependent ^{1}H-NMR and X-ray analysis confirmed the locked sugar structure and revealed a preference for the 1′-exo/2′-endo conformation as well as for the pseudoequatorial position of the secondary 5′-oxo-substituent (Fig. 1). While the furanose conformation thus strongly resembles that of B-type DNA, the conformation around the C(4′)–C(5′) bond (torsion angle γ) differs by ~100° from that found in DNA duplexes of the A- and B-type. These well defined geometric alterations in the repetitive bicyclo-DNA backbone unit relative to that of natural DNA prompted us to investigate in detail its consequences on the duplex structures formed by bicyclo-DNA. As a result, we could
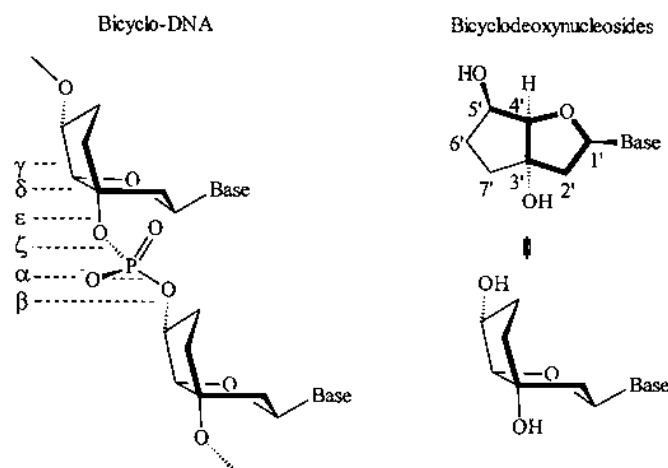
Figure 1. The structure of bicyclo-DNA and the bicyclonucleosides including representation of their preferred conformation.

*To whom correspondence should be addressed. Tel: +41 31 631 4355; Fax: +41 31 631 3422; Email: leumann@ioc.unibe.ch

[+]Present address: Laboratory of Organic Chemistry, ETH-Zürich, Universitätstrasse 16, CH-8092 Zürich, Switzerland

show that homopurine/homopyrimidine sequences form very stable duplexes of the Hoogsteen and reverse Hoogsteen type under specific A·T and C$^+$·G base pair formation (9).

Specific recognition of single-stranded DNA or RNA of any base sequence by an oligonucleotide, however, requires the Watson–Crick base pairing mode. Here we report on the Watson–Crick base pairing properties of bicyclo-DNA sequences, 6–12 nucleotides in length, containing all four natural DNA bases with complementary RNA, DNA and with itself, as well as their resistance against nucleases.

MATERIALS AND METHODS (ref. 10)

Synthesis and characterization of oligo-bicyclodeoxy-nucleotides

The synthesis of the bicyclodeoxynucleosides, the corresponding cyanoethyl phosphoramidites (and allyl phosphoramidite in the case of bicyclothymidine) for oligonucleotide assembly as well as the starter units bound to the solid support is described elsewhere (5,7). Automated bicyclo-DNA synthesis was performed on a Pharmacia LKB Gene Assembler Special DNA synthesizer on a 1.0–1.5 μmol scale using the modified protocol for bicyclo-DNA assembly, allowing for a prolonged coupling (6 min) and detritylation (60 s) time relative to the synthesis of natural DNA oligomers (7). Coupling yields were in the range of 98% per step.

End-detritylated oligonucleotides were detached from solid support and frayed from protecting groups by standard deprotection (25% aq. NH₃, 55°C, 10–20 h). In the cases where allyl phosphoramidites were used, Pd(0) catalyzed allyl deprotection according to the method of Hayakawa *et al*. (11) preceded the ammonia treatment. Purification was performed by HPLC (Pharmacia LKB 2249 gradient pump, UV-detection 260 nm) on reversed phase stationary phase (Aquapore RP 300, 220 × 4.6 mm, Brownlee, linear gradient of max. 80% CH₃CN in 0.1 M aq. triethylammonium acetate, pH 7.0) and anion exchange stationary phase (Nucleogen DEAE 60-7, Macherey&Nagel, linear gradient of max. 1 M KCl in 20 mM NaH₂PO₄, pH 6.0, H₂O:CH₃CN 4:1; or Mono Q HR 5/5, Pharmacia, linear gradient of max. 1 M NaCl in 10 mM aq. NaOH).

The isolated oligonucleotides were desalted over SEP-PAK cartridges (Waters). The homogeneity of the collected fractions was additionally secured in the case of the sequences bcd(CGCGA-ATTCGCG) and bcd(GCGAATTGCG) by capillary electrophoresis (Waters Quanta 4000, capillary: J&W Scientific (Fisons), 75cm × 75μm, polyacrylamide gel filled (5%T, 5%C), buffer: 100 mM Tris-borate, 7 M urea, pH 8.3). All bicyclo-deoxyoligonucleotides, with the exception of bcd(G₆), were analyzed by MALDI-TOF mass spectrometry as described (12) and were within 2% of the expected mass (monoanionic form). Analytical data as well as yields for the bicyclo-oligomers used in this study are in the supplementary material.

Natural oligodeoxynucleotides containing bicyclo-deoxynucleosides were synthesized according to standard phosphoramidite chemistry using the modified cycle, described above, for the introduction of the modified nucleosides only. Oligoribonucleotides were prepared as described (13) (coupling time, 17 min), purified by HPLC (DEAE anion exchange) and desalted over Sephadex G-10 (BioRad).

Enzyme digestions

Enzyme digestions of oligonucleotides were performed by treating 1.25 ml of a solution containing 1.5 OD₂₆₀ oligonucleotide in 180 mM NaCl, 12 mM Tris–HCl, pH 7.0 at 37°C with 6 mU of snake venom phosphodiesterase and 125 U of alkaline phosphatase (Boehringer, Mannheim) and followed by recording the increase in UV-absorption (260 nm) as a function of time. Half life times (Table 4) were directly determined from these curves.

Extinction coefficients of oligo-bicyclodeoxynucleotides

Extinction coefficients of oligo-bicyclodeoxynucleotides were obtained from the same enzyme hydrolysis curves according to the general formula

$$\epsilon(oligo) = \frac{\text{abs}_{260}(\text{start})}{\text{abs}_{260}(\text{end})} \cdot \sum_{i=1}^{n} \epsilon_i(mono)$$

where abs₂₆₀(start) means the initial absorption, abs₂₆₀(end) the absorption after complete digestion of the oligomer and ε(*mono*) the experimentally determined extinction coefficient of the bicyclo-deoxynucleosides at 260 nm (bcd(A) = 13700, bcd(C) = 6200, bcd(G) = 10700, bcd(T) = 8700). Completeness of digestion of the oligomers to the free nucleosides was reassured by reversed phase HPLC analysis (vide supra) and identification of the products by coinjection with authentic material. Extinction coefficients for natural DNA oligomers were calculated as described (14).

UV-melting curves

UV-melting curves were measured on a Varian Cary 3E UV/VIS spectrophotometer equipped with a temperature controller and a multi cell peltier block, interfaced to a Compaq ProLinea 3/25 ZS computer. A temperature gradient of 0.5°C/min was applied and a heating–cooling–heating cycle was used. At temperatures below 15°C, the cell compartment was flushed with nitrogen to prevent condensation of water on the cuvettes. Sample solutions were covered with a thin layer of dimethylpolysiloxane (Sigma) in order to prevent evaporation of water. In all cases, heating and cooling curves were superimposable indicating reversible equilibrium conditions. T_m data were defined as the maxima of the first order derivative of the melting curves and were shown to correspond within ±1°C to those determined at half of the maximal hyper-chromicity after baseline correction. Thermodynamic data for duplex formation were obtained as described (15).

CD-spectra

CD spectra were recorded on a Jasco J-500A spectropolarimeter connected to a PC via a IF-500 II (Jasco) interface. Temperature was controlled by a Julabo F20 circulating bath and measured directly in the cell (path length 10 mm).

RESULTS

Complementary base-pairing of bicyclo-DNA with natural DNA and RNA

We synthesized a series of bicyclo-DNA sequences and analyzed their binding affinities to complementary DNA and RNA by UV-melting curves. All duplex melting curves reflect highly cooperative melting transitions and are completely reversible. Dominant self aggregation phenomena of the single strands could

be excluded in all cases. T_m data and sequences of the hybrid duplexes investigated are reproduced in Table 1. Inspection of the data leads to a picture in which replacement of purine-rich sequences by bicyclo-DNA decrease duplex stability whereas replacement of pyrimidine-rich DNA sequences by bicyclo-DNA does not. As often observed, complementary base-pairing with RNA is more efficient as with DNA. Structures of hybrid duplexes with complementary RNA were followed by CD-spectroscopy in the case of the sequence bcd(GGATGGGAG) and bcd(CTCCC-ATCC). These spectra are similar to that of the corresponding all RNA duplex (Fig. 2). Small but clear differences arise in the relative ellipticities in the region near to the maximum positive cotton effect at 270 nm.

Complementary Watson–Crick base pairing between bicyclo-DNA strands

Duplexes of varying length and base composition were analyzed by UV-melting curves. The concomittant analysis of the same sequences in natural DNA thereby allowed for a direct comparison of the two backbone systems. In the selection of the base sequences we were guided mostly by structural considerations. The nonamer duplex d(GGATGGGAG)·d(CTCCCATCC), corresponding to the central part of the binding site of the transcription factor IIIA, was shown to adopt an A-conformation in the crystalline state (16) and a partial A-conformation in solution as inferred from CD-spectroscopy (17). The self-complementary d(CGCGAATTCGCG) on the other hand is known to adopt a B-conformation in the crystal (18) and in solution (19). Table 2 gives an overview of the results in the bicyclo-DNA series and presents comparisons with natural DNA in the case of identical antiparallel matched sequences. CD spectra of the bicyclo-DNA nonamer duplex **A** in comparison with the corresponding DNA duplex are depicted in Figure 2.

Table 1. T_m and (ΔT_m/mod.)-data of bicyclo-DNA–DNA and bicyclo-DNA–RNA hybrid duplexes

	DNA complement[a]		RNA complement[b]	
	$T_m^{(280\ nm)}$ [°C]	ΔT_m/mod	$T_m^{(260\ nm)}$ [°C]	ΔT_m/mod[c]
bcd(GGATGGGAG)	23.9	–1.7	31.7	–0.8
d(GGATGGGAG)	39.2	0	39.2	0
bcd(CTCCCATCC)	35.3	–0.4	42.1	+0.3
d(CTCCCATCC)	39.2	0	38.6	–0.1
bcd(CCCCCC)	32.5	+0.3	–	–
d(CCCCCC)	30.7	0	–	–
bcd(GGGGGG)	16.2	–2.4	30.5[d]	–2.1[d]
d(GGGGGG)	30.7	0	43.0[d]	0[d]

[a]4.4–6.8 µM duplex in 150 mM NaCl, 10 mM Tris–HCl, pH 7.0.
[b]4.9–5.7 µM duplex in 150 mM NaCl, 10 mM NaH_2PO_4, pH 6.5, wild type (all RNA) duplex: T_m = 51.0°C.
[c]Values relative to RNA–DNA duplex.
[d]Poly(C) was used as RNA complement [c = 34 µM in base-pair; buffer as b) but pH 8.3]. T_m determined at 280 nm.
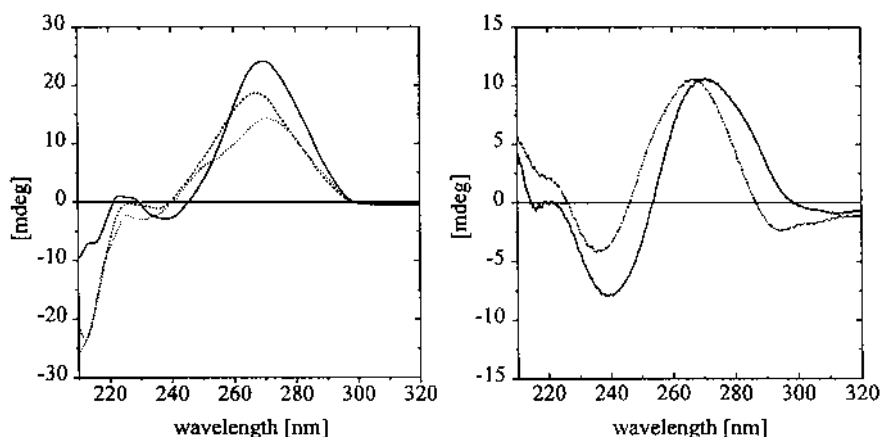
Figure 2. Left: CD curves (10°C) of bcd(GGATGGGAG)·r(CUCCCAUCC), (···); r(GGAUGGGAG)·r(CUCCCAUCC), (---); r(GGAUGG-GAG)·bcd(CTCCCATCC), (—); in 10 mM NaH_2PO_4, 150 mM NaCl, pH 6.5; oligonucleotide conc. = 5.0–5.7 µM; Right: the corresponding CD spectra of the natural DNA (—) and bicyclic duplex (…) (c = 5–6 µM, 4°C, 10 mM Tris–HCl, 150 mM NaCl, pH 7.0).
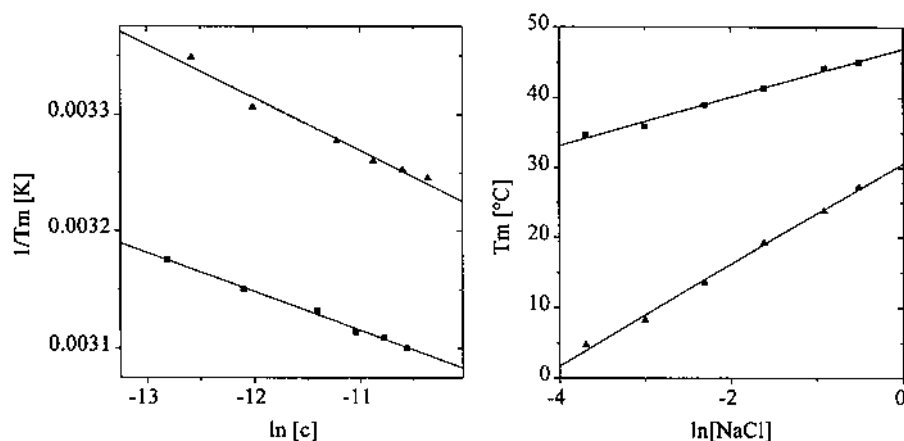
Figure 3. Left: plot of $1/T_m$ versus ln[c] (10 mM NaH_2PO_4, 1 M NaCl, pH 7.0, c = 2.7–31.7 μM), Right: plot of T_m versus ln [NaCl] (10 mM NaH_2PO_4, pH 7.0, c = 5.0 μM, 0.025–0.6 M NaCl) for the duplex sequence 5'-GGATGGGAG)-3'·5'-CTCCCATCC-3' in the natural (■) and the bicyclo-DNA (▲) series.

Table 2. T_m data (c = 4.4–6.0 μM) of bicyclo-DNA duplexes in comparison with natural DNA

Entry	Sequence	T_m (280 nm) [°C][a]	
		bicyclo-DNA	DNA
A	5'-GGATGGGAG		
	CCTACCCTC-5'	(18.1[b]), 30.9	(39.2[b]), 43.6
B	5'-GGAAGGGAG		
	CCTTCCCTC-5'	30.5	
C	5'-GGATGGGAG		
	5'-CCTACCCTC	<0	
D	5'-GGA**A**GGGAG		
	CCT**A**CCCTC-5'	<5	
E	5'-GGA**T**GGGAG		
	CCT**T**CCCTC-5'	12.2	
F	5'-GGGGGG		
	CCCCCC-5'	22.5[b]	30.7[b]
G	5'-CGCGAATTCGCG[e]	75.8[c]	64.2[c]
H	5'-GCGAATTCGC[e]	70.0[c]	
I	5'-CGAATTCG	<0[d]	

[a]10 mM NaH_2PO_4, 1 M NaCl, pH 7.0.
[b]10 mM Tris–HCl, 150 mM NaCl, pH 7.0.
[c]10 mM NaH_2PO_4, 100 mM NaCl, pH 7.0.
[d]1 mM NaH_2PO_4, 10 mM NaCl, pH 7.0.
[e]Monomolecular hairpin duplex.

Comparison of the T_m data of the bicyclo-DNA and the natural DNA nonamer duplex (Table 2, entry A) reveals a thermodynamic advantage of the latter. Within the bicyclo-DNA sequence, conversion of a central T·A to a A·T base pair (Table 2, entry B) did not affect duplex stability indicating that there is no notable energetic difference between Watson–Crick base pairing in a oligopurine–oligopyrimidine sequence compared with one containing both purines and pyrimidines in one strand. As in the case of natural DNA, bicyclo-DNA strongly prefers the antiparallel pairing arrangement. This can be deduced from the melting experiment with the two parallel complementary bicyclo-DNA sequences (Table 2, entry C) in which no cooperative transition >0°C could be observed. Another feature investigated was the ability of bicyclo-DNA to discriminate between mismatches. As can be seen from the corresponding T_m data (Table 2, entries D and E), neither an A·A nor a T·T mismatch is tolerated. Both arrangements lead to a decrease of T_m of at least 18.7°C relative to the matched duplex. We also determined the base-pairing properties of the hexameric complementary oligomers bcd(G_6) and bcd(C_6), the former sequence being of special interest by itself due to its propensity for quadruplex formation via G-tetrads in the case of DNA (20–22). In contrast to the natural sequence d(G_6), no cooperative transition but signs of the formation of unspecific aggregates at low temperatures (0 to –20°C) were observed. Complementary base-pairing of bcd(G_6) with bcd(C_6) (Table 2, entry F), however, occurred but was again less efficient compared with the DNA duplex (ΔT_m of –8.2°C).

The CD spectra of the bicyclic and the natural nonamer duplexes corresponding to the sequence entry A (Fig. 2) are similar in nature. While the positive maxima around 270 nm are equal in amplitude, the minimum near 240 nm is slightly less pronounced in the bicyclo-DNA duplex compared with its natural equivalent. Thus the CD spectra confirm the presence of a Watson–Crick duplex in the case of bicyclo-DNA.

The thermodynamic characteristics of duplex formation for the natural and the bicyclic sequence A were determined by a plot of $1/T_m$ versus ln [c] (Fig. 3). Comparison of the data for both systems (Table 3) clearly shows an enthalpic advantage for duplex formation in the natural system and an entropic advantage for the bicyclic system. The changes of ΔH and ΔS are compensatory in nature, and the calculated free enthalpy of duplex formation ($\Delta G^{25°C}$) is in favor of a higher stability of the natural duplex as expected from the T_m values.

Table 3. Thermodynamic data for duplex formation of a bicyclo-DNA nonamer in comparison with the analogous natural DNA nonamer

	ΔH	ΔS	$\Delta G^{25°C}$	$\dfrac{\delta Tm}{\delta(1n[NaCl])}$	Δn
	[kcal·mol^{-1}]	[cal·K^{-1}·mol^{-1}]	[kcal·mol^{-1}]		
bcd(GGATGGGAG)·bcd(CTCCCATCC)	−42.4 ± 3.1	−114 ± 9	−8.4	7.2 ± 0.2	3.3
d(GGATGGGAG)·d(CTCCCATCC)	−60.4 ± 2.6	−163 ± 7	−11.8	3.5 ± 0.2	2.1

10 mM NaH$_2$PO$_4$, 1 M NaCl, pH 7.0

We also investigated the influence of electrolyte concentration on duplex stability by varying the salt concentration (NaCl) in the buffer (Fig. 3; Table 3). As expected, in both cases a linear dependence of T_m from ln([NaCl]) was observed. T_m values are much more variable in the case of the bicyclic duplex than in the natural one. The differences amount to 22.5°C (0.025–0.6 M NaCl) in the bicyclic case, compared with 10.5°C for the natural duplex in the same concentration range. According to the polyelectrolyte theory (23,24) we determined the relative counter ion uptake (Δn) on the basis of the experimentally determined values for ΔH and $\delta T_m/\delta$ln([NaCl]) for both duplexes according to the formula

$$\delta n = -\frac{2\delta H}{RTm^2} \cdot \frac{\delta Tm}{\delta(1n[NaCl])}$$

Upon duplex formation, the bicyclic system screens more counter ions from the solvent than the natural one (Table 3). The differential uptake amounts to one additional positive charge per ~7 base pairs relative to the natural system.

In the light of the generally lower stability of bicyclo-DNA duplexes it was initially a surprise to find that the self complementary bicyclo-DNA dodecamer of the sequence 5′-CGCGAATTCGCG-3′ shows a melting transition with a T_m that is higher by 11.3°C compared with the natural sequence (Table 2, entry G). We therefore determined the molecularity of the transition in the bicyclic system by concentration dependent T_m measurements. At 100 mM NaCl no dependence of the T_m over an oligonucleotide concentration range of 3.0–24.4 μM was observed (10 mM NaH$_2$PO$_4$, 100 mM NaCl, pH 7.0; T_m = 75.5 ± 0.6°C). The same is also true for sodium chloride concentrations as high as 1 M (10). This confirms that in contrast to natural DNA (25), this particular sequence adopts only a monomolecular hairpin duplex structure in bicyclo-DNA.

In order to determine the minimal requirements of the stem length in this bicyclic hairpin duplex, we prepared the corresponding deca- and octamer having a reduced stem length by one and two base-pairs respectively (Table 2, entries H and I). While the decamer still exhibits a strongly cooperative melting transition with a T_m of 70.0°C, the octamer appears only as a non-paired single strand at temperatures above 20°C. Thus the minimal required stem size necessary for stable hairpin formation are three G·C (C·G) base pairs in this stem–loop system. Interestingly, the hairpins of the dodecamer G and the decamer H are of similar stability (ΔT_m = 5.5°C).

Left-handed bicyclo-DNA?

On the basis of the self-complementary hexamer sequence (CG)$_3$ we investigated the influence of bicyclodeoxynucleotides on its possibility to undergo a salt induced B→Z conformational transition by CD-spectroscopy. While under neutral conditions (10 mM Tris–HCl, pH 7.0), the natural duplex d(CG)$_3$ (10 μM, T_m = 46.2°C, 0.15 M NaCl) clearly switches to a Z conformation upon raising the NaCl concentration from 0.15 to 4 M, substitution of bicyclo-deoxycytidine for deoxycytidine [(bcdC-dG)$_3$, 10 μM, T_m = 51.0°C, 0.15 M NaCl], or bicyclo-deoxyguanosine for deoxyguanosine [(dC-bcdG)$_3$, 10 μM, T_m = 51.4°C, 0.15 M NaCl] completely abolishes this conformational transition (Fig. 4). No doubt that also the completely bicyclic duplex bcd(CG)$_3$ (10 μM, T_m = 38.5°C, 0.15 M NaCl) showed no tendency to adopt a left handed Z-conformation either.

The fact that any substitution of a bicyclo-deoxynucleoside for a deoxynucleoside in the left handed DNA forming sequence (CG)$_3$ abolishes Z-DNA formation is not unexpected and can be explained with the inability of the bicyclo-G nucleoside to adopt a 3′-endo furanose conformation and the bicyclo-C nucleoside to adopt a synclinal conformation around the C(4′)-C(5′) bond (torsion angle γ) as required for Z-DNA formation (26).

Enzymic stability of bicyclo-DNA

We specified the degree of resistance of bicyclo-DNA towards the stability of 3′ exonucleases, the latter being mostly responsible for nucleolytic degradation of oligonucleotides in plasma (27). The sequences shown in Table 4 were subjected to hydrolysis catalyzed by the 3′-exonuclease snake venom phosphodiesterase and the corresponding half-life times determined by UV-spectroscopy.

Table 4. Half-life times ($t_{1/2}$) of bicyclo-DNA sequences in the presence of the enzyme snake venom phosphodiesterase in comparison with natural DNA oligomers

Sequence	$t_{1/2}$ [min] (c = μM)	
	Bicyclo–DNA	DNA
5′-GGATGGGAG	32 (15.4)	≤ 3 (13.1)
5′-GGAAGGGAG	66 (16.3)	–
5′-CTCCCTTCC	84 (25.4)	–
5′-CCTACCCTC	112 (18.9)	–
5′-CTCCCATCC	68 (23.1)	≤ 3 (17.3)
5′-CGCGAATTCGCG	196 (17.7)	15 (9.2)

The half-life times were in the range of 30–200 min under the conditions chosen for the assay. For the cases where a direct comparison with the natural DNA oligomers was possible, an increased stability of bicyclo-DNA by a factor of 10–20 was determined.

The DNA sequence d(CGACTATGCAAcccc), bearing a 3′-end consisting of four consecutive bicyclodeoxycytidine (c) residues (T_m with complementary RNA, 57.1°C; ΔT_m/mod. versus DNA/RNA wild type = –0.5°C; 10 mM NaH$_2$PO$_4$, 0.1 M NaCl, 0.1 mM
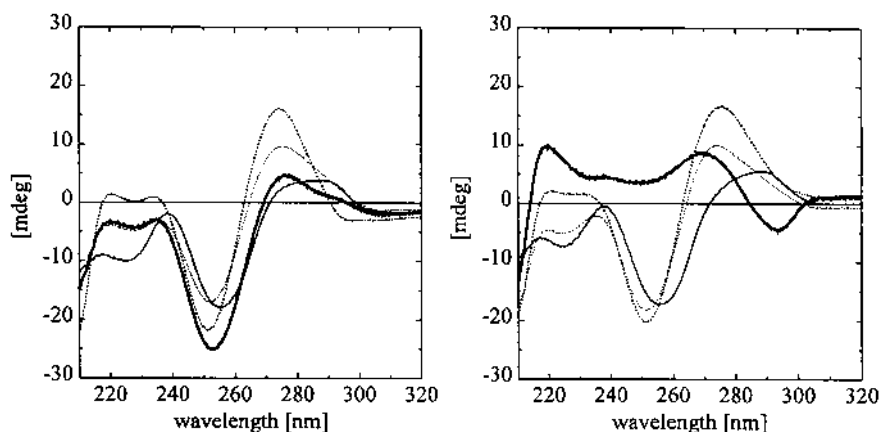
Figure 4. CD spectra of the self-complementary duplexes d(CG)$_3$ (–); (dC-bcdG)$_3$ (—); (bcdC-dG)$_3$ (---) and bcd(CG)$_3$, (···) in 10 mM Tris–HCl, pH 7.0, 4°C, c = 10 μM. Left: 0.15 M NaCl; Right 4 M NaCl.
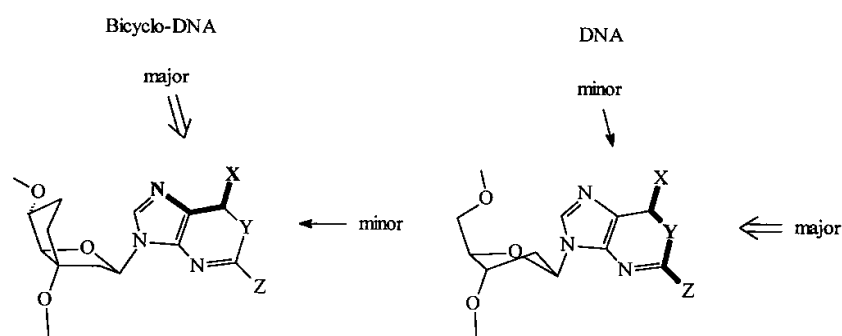
Figure 5. Purine bases preferentially accept a complementary base on the Hoogsteen side in bicyclo-DNA and on the Watson–Crick side in natural DNA.

EDTA, pH 7.0) was used for an additional assay of enzymic resistance in a medium containing 10% heat deactivated fetal calf serum (28). The half-life of the bicyclonucleoside modified sequence (specified as the disappearance of the full length oligonucleotide from *n* to *n* – 1) was determined to be 4 h, corresponding to an 8-fold enhancement in nuclease stability relative to the all DNA control sequence.

DISCUSSION

Effects of the bicyclo-DNA backbone on Watson–Crick duplex stability

From the sequences investigated it appears that Watson–Crick duplexes made entirely of bicyclonucleotides are distinctly less stable compared with those in the natural DNA series. The stability of bicyclo-DNA–DNA or bicyclo-DNA–RNA duplexes follow the same trend especially if purine-rich bicyclo-DNA sequences are involved. This compares inversely proportional to the relatively high stability of Hoogsteen base-paired bicyclo-DNA duplexes (9) and supports the view that bicyclo-DNA purine nucleotides, in contrast to natural DNA, preferentially accept complementary strands at the Hoogsteen face of the nucleobases and not at the Watson–Crick face (Fig. 5)—this as a direct consequence of the structural alteration of the backbone within torsion angle γ.

Duplex stability in bicyclo-DNA is strongly dependent on the ratio of G·C versus A·T base pairs. Under comparable conditions (0.15 M NaCl) the hexamer duplex bcd(GGGGGG)· bcd(CCCCCC) is of equal thermal stability as the nonamer duplex bcd(GGATGGGAG)·bcd(CTCCCATCC) (Table 2). Since the latter duplex can be regarded as an extended form of the former, to which two A·T and a T·A base pair were added, one can deduce that the stability of Watson–Crick duplexes in bicyclo-DNA is dominated by the number of G·C base pairs. A·T base pairs seem to neither positively nor negatively (compare mismatched sequences in Table 2) contribute to the overall stability and thus seem to behave energetically neutral. This, again, complements earlier results with bicyclo-DNA sequences of the bases A and T, where the alternating decamer bcd(AT)$_5$ (restricted to Watson–Crick pairing by sequence) fails to base pair at all while duplexes of bcd(A$_{10}$)·bcd(T$_{10}$), which occur in the Hoogsteen and/or reversed Hoogsteen mode, are very stable (9). Nearest neighbor effects on A·T base pair stability may also be of importance. However, they were not systematically addressed in this report.

The fact that A·T base pairs are of low energetic reward in duplex formation also explains the preferential monomolecular hairpin structure of the self-complementary dodecamer sequence bcd(CGCGAATTCGCG), in which presumably the A–A–T–T part is located in the loop, while the stem is held together by four C·G base pairs. The higher thermodynamic stability relative to the natural dodecamer, however, cannot be the consequence of stronger G·C base pairs in bicyclo-DNA since both the duplexes

bcd(GGGGGG)·bcd(CCCCCC) and bcd(CG)$_3$ are less stable than their natural equivalents. Obviously bicyclonucleotides are stabilizing the loop of the hairpin presumably due to their reduced structural flexibility and/or their preferred geometry of the backbone.

Thermodynamic properties

We have reported earlier that duplex formation in the bcd(A$_{10}$)·bcd(T$_{10}$) series is entropically favored and enthalpically disfavored with respect to the corresponding natural duplex and thus seems to be a general property of bicyclo-DNA (6,7). However, since the bicyclic duplex is Hoogsteen or reversed Hoogsteen base paired (9) and the natural one Watson–Crick base paired, this comparison needed a further confirmation on the basis of a sequence, that adopts the same (Watson–Crick) duplex constitution in both systems. These prerequisites were given with the sequence A (Table 2). Assuming validity of the two state dissociation model, the thermodynamic data obtained from UV-melting curves (Table 3) show the same trend: loss of pairing enthalpy and gain of pairing entropy. Again, we attribute the enthalpic loss to strain in the duplex caused by the structural alterations around torsion angle γ in bicyclo-DNA, and the entropic gain, at least in part, to the reduced flexibility of the sugar–phosphate backbone. To what extent differential solvation of the backbones in DNA and bicyclo-DNA affects the entropy term is unknown so far.

The higher dependence of duplex formation from monovalent cation concentration relative to natural DNA seems to be independent of the base sequence and association mode and seems to be a general property of the altered backbone structure in bicyclo-DNA. This has already been observed in bicyclo-DNA Hoogsteen duplexes (7) as well as in duplexes formed in the α-bicyclo-DNA series (30,31). In all cases the number of counter ions screened from the solvent is higher with respect to the corresponding natural duplexes. This higher demand may have its origin in the additional ethylene bridge that directly perturbs solvation of the phosphate groups, or more likely, in an extended conformation of the bicyclo-DNA single strands compared with the natural ones (assuming that intrastrand phosphate distances in the stacked duplexes are about equal in both systems).

Enzymic stability

The linking phosphodiester groups in bicyclo-DNA are higher substituted than in natural DNA. One would therefore expect this unit to be less of a substrate for enzymic degradation than that of natural DNA. Much to our surprise, however, bicyclo-DNA is only moderately more stable against 3′ exonucleases (Table 4). The stability against snake venom phosphodiesterase (SVP) is slightly dependent from the base sequence and, as in the case of natural DNA, seems to be moderately higher in the case of duplexed sequences with respect to single strands as deduced from the self-complementary dodecamer 5′-CGCGAATTCGCG-3′ in both backbone systems. In general terms, modifications on the α-side of the natural nucleosides [as in α-DNA (32,33), α-bicyclo-DNA (30,31) or 2′-O-alkyl-RNA (34)] seem to increase the enzymic stability more efficiently than the modifications on the β-side in bicyclo-DNA. The moderately enhanced 3′-exonuclease stability of bicyclo-DNA is also reflected in the serum experiment with the DNA sequence containing a 3′-bicyclo-deoxynucleotide cap.

CONCLUSIONS

The results presented here, together with earlier findings on Hoogsteen and reversed Hoogsteen pairing of oligopurine/oligopyrimidine strands in bicyclo-DNA (9), now allow for a generalized description of the differences in the association properties within the two pairing systems (bicyclo-DNA and natural DNA).

(i) Bicyclo-DNA strongly prefers the Hoogsteen association mode and discriminates the Watson–Crick association mode and thus behaves opposite to what is known from natural DNA. Furthermore, bicyclo-DNA Hoogsteen and reversed Hoogsteen duplexes are of higher thermodynamic stability relative to the Watson–Crick duplex of natural DNA for a given purine sequence motif (9). (ii) Within the Watson–Crick pairing regime both, natural and bicyclo-DNA strongly prefer antiparallel over parallel strand alignment and discriminate base–base mismatches. (iii) Bicyclo-DNA, however, does not discriminate between the parallel (Hoogsteen) and the antiparallel (reversed Hoogsteen) arrangement upon duplex formation and thus behaves differently from natural DNA for which a parallel Hoogsteen duplex was reported (35), but for which the antiparallel reversed Hoogsteen pairing-mode is only described in the context of DNA triple helix formation by oligopurine strands (36) or oligomers containing deoxyguanosine and thymidine (37).

Besides serving as a model for the study of structure/association mode relations in DNA, bicyclo-DNA also shows interesting antisense properties. Due to their strong pairing and enhanced nuclease stability, pyrimidine rich bicyclo-DNA sequences can advantageously be used in the recognition of single-stranded RNA. Furthermore bicyclothymidine is an efficient substitute for natural thymidine in DNA duplex recognition by oligonucleotides. We have shown earlier that substitution of bicyclothymidine for thymidine in a pyrimidine DNA sequence exerts a stabilizing effect on triple helix formation in the parallel binding motif (29).

ACKNOWLEDGEMENTS

REFERENCES

1 Wagner,R.W. (1994) *Nature*, **372**, 333–335.
2 Milligan,J.F., Matteucci,M.D. and Martin,J.C. (1993) *J. Med. Chem.,* **36**, 1923–1937.
3 De Mesmaeker,A., Häner,R., Martin,P. and Moser,H.E. (1995) *Acc. Chem. Res.,* **28**, 366–374.
4 Thuong,N.T. and Hélène,C. (1993) *Angew. Chem. Intl. Ed. Engl.*, **32**, 666–690.
5 Tarköy,M., Bolli,M., Schweizer,B. and Leumann,C. (1993) *Helv. Chim. Acta*, **76**, 481–510.
6 Tarköy,M. and Leumann,C. (1993) *Angew. Chem. Intl. Ed. Engl.,* **32**, 1432–1434.
7 Tarköy,M., Bolli,M. and Leumann,C. (1994) *Helv. Chim. Acta*, **77**, 716–744.
8 Egli,M., Lubini,P., Bolli,M., Dobler,M. and Leumann,C. (1993) *J. Am. Chem. Soc.*, **115**, 5855–5856.
9 Bolli,M., Litten,C., Schütz,R. and Leumann,C. (1996) *Chem. Biol.*, **3**, 197–206.
10 Bolli,M. (1994) Nukleinsäure-Analoga mit Konformationell Eingeschränktem Zucker-Phosphat-Rückgrat ('Bicyclo-DNA'): Synthese und Eigenschaften. Dissertation, University of Bern.

11 Hayakawa,Y., Wakabayashi,S., Kato,H. and Noyori,R. (1990) *J. Am. Chem. Soc.,* **112**, 1691–1696.

12 Pieles,U., Zürcher,W., Schär,M. and Moser,H.E. (1993) *Nucleic Acids Res.,* **21**, 3191–3196.

13 Usman,N., Ogilvie,K.K., Jiang,M.-Y. and Cedergren,R.J. (1987) *J. Am. Chem. Soc.,* **109**, 7845–7854.

14 Fasman,C.R. (1975) *Handbook of Biochemistry and Molecular Biology,* 3rd Edn. CRC Press, Cleveland, OH, p. 589.

15 Marky,L.A. and Breslauer,K.J. (1987) *Biopolymers*, **26**, 1601–1620.

16 McCall,M., Brown,T., Hunter,W.N. and Kennard,O. (1986) *Nature*, **322**, 661–664.

17 Fairall,L., Martin,S. and Rhodes,D. (1989) *EMBO J.*, **8**, 1809–1817.

18 Drew,H.R., Wing,R.M., Takano,T., Broka,C., Tanaka,S., Itakura,K. and Dickerson,R.E. (1981) *Proc. Natl. Acad. Sci. USA*, **78**, 2179–2183.

19 Hare,D.R., Wemmer,D.E., Chou,S.-H., Drobny,G. and Reid,B.R. (1983) *J. Mol. Biol.,* **171**, 319–336.

20 Smith,F.W. and Feigon,J. (1992) *Nature*, **356**, 164–168.

21 Kang,C., Zhang,X., Ratliff,R., Moyzis,R. and Rich,A. (1992) *Nature*, **356**, 126–131.

22 Laughlan,G., Murchie,A.I.H., Norman,D.G., Moore,M.H., Moody,P.C.E., Lilley,D.M.J. and Luisi,B. (1994) *Science*, **265**, 520–524.

23 Manning,G.S. (1978) *Q. Rev. Biophys.*, **11**, 179–246.

24 Record,M.T.,Jr. Anderson,C.F. and Lohman,T.M. (1978) *Q. Rev. Biophys.*, **11**, 103–178.

25 Marky,L.A., Blumenfeld,K.S., Kozlowski,S. and Breslauer,K.J. (1983) *Biopolymers*, **22**, 1247–1257.

26 Saenger,W. (1984) *Principles of Nucleic Acid Structure*. Springer-Verlag, New York.

27 Eder,P.S., DeVine,R.J., Dagle,J.M. and Walder,J.A. (1991) *Antisense Res. Dev.*, **1**, 141–151.

28 Hoke,G.D., Draper,K., Freier,S.M., Gonzalez,C., Driver,V.B., Zounes,M.C. and Ecker,D.J. (1991) *Nucleic Acids Res.*, **19**, 5743–5748.

29 Bolli,M. and Leumann,C. (1995) *Angew. Chem. Intl. Ed. Engl.,* **34**, 694–696.

30 Bolli,M., Lubini,P., Tarköy,M. and Leumann,C. (1994) In Sanghvi,Y.S. and Cook,P.D. (eds), *Carbohydrate Modifications in Antisense Research*. ACS Symposium Series, 580, Washington, DC, pp. 100–117.

31 Bolli,M., Lubini,P. and Leumann,C. (1995) *Helv. Chim. Acta*, **78**, 2077–2096.

32 Morvan,F., Rayner,B., Imbach,J.-L., Thenet,S., Bertrand,J.-R., Paoletti,J., Malvy,C. and Paoletti,C. (1987) *Nucleic Acids Res.*, **15**, 3421–3437.

33 Cazenave,C., Chevrier,M., Thuong,N.T. and Hélène,C. (1987) *Nucleic Acids Res.*, **15**, 10507–10521.

34 Sproat,B.S., Lamond,A.I., Beijer,B., Neuner,P. and Ryder,U. (1989) *Nucleic Acids Res.,* **17**, 3373–3386.

35 Liu,K., Miles,H.T. and Sasisekharan,V. (1993) *Biochemistry,* **32**, 11802–11809.

36 Durland,R.H., Kessler,D.J., Gunnell,S., Duvic,M., Pettitt,B.M. and Hogan,M.E. (1991) *Biochemistry*, **30**, 9246–9255.

37 Sun,J.S., De Bizemont,T., Duval-Valentin,G., Montenay-Garestier,T. and Hélène,C. (1991) *C.R. Acad. Sci. Paris Ser III*, **313**, 585–590.